Pharmaceutical Research, Vol. 24, No. 8, August 2007 (© 2007)
DOI: 10.1007/s11095-007-9266-8

Research Paper

Longitudinal Analysis of Gene Expression in Porcine Skeletal Muscle After Post-Injection Local Injury

Pierre J. Ferré,[1] Laurence Liaubet,[2] Didier Concordet,[1] Magali SanCristobal,[2] Emmanuelle Uro-Coste,[3] Gwenola Tosser-Klopp,[2] Agnès Bonnet,[2] Pierre-Louis Toutain,[1] François Hatey,[2] and Hervé P. Lefebvre[1,4]

Received September 20, 2006; accepted February 7, 2007; published online March 23, 2007

Purpose. The purpose of this study is to describe the time course of gene expression in a skeletal muscle local injury induced by an intramuscular (IM) injection, and to compare the dynamics of gene expression with pathological events.
Materials and Methods. Ten piglets received 4 IM injections of propylene glycol in the longissimus dorsi muscles 6 h, 2, 7, and 21 days before euthanasia, where control and injected muscle sites were sampled for RNA isolation and microscopic examination. The hybridization of nylon cDNA microarrays was carried out with radioactive probes obtained from the muscle RNA.
Results. 153 genes were found under- or over-expressed at least once among the investigated time-conditions. The eight most discriminant genes were also identified: Two genes (GTP-binding protein RAD and Ankyrin repeat domain protein) were over-expressed at 6 h and six genes between 2 and 21 days (Osteonectin, Fibronectin, Matrix metalloproteinase-2, Collagen alpha 1(I) chain, Collagen alpha 2(I) chain, and Thymosin beta-4). Necrosis, inflammation and regeneration were observed through both the dynamics of gene expression profiles and through the microscopic examinations.
Conclusion. Our data demonstrate that several pathways are involved in post-injection muscle injury, and that necrosis, inflammation and regeneration are not sequential but occur in parallel.

KEY WORDS: gene expression profiling; injury; intramuscular injection; local tolerance; pathophysiology.

INTRODUCTION

The intramuscular (IM) route is widely used for drug administration. It has been formerly estimated that more than half a million IM injections are administered daily within the US (1). It was also observed by the Boston Collaborative Drug Surveillance Program that 46% of patients received at least one IM injection during hospitalization. Adverse events were observed after 0.4% of the total number of IM administrations (2), with skeletal muscle injury and patient discomfort or pain. More recently, a survey showed that 23% of 639 pediatric nurses had observed serious complications after the IM injections they had performed (3). An IM injection is mainly associated with pain, swelling, redness and movement discomfort. Chronic effects with local fibrosis of the muscles leading to muscle contractures (4,5), and abscesses (6) or Staphylococcus aureus sepsis (7) have also been observed. Macrophagic myofasciitis, an emerging medical pathology, has been described and hypothetically associated with the IM injection of vaccinal drugs (8).

The basic gross and microscopic pathologic examinations carried out during the development of a drug formulation for IM use allow rough evaluation of the extent and severity of muscle lesions in connection with the drug, vehicle, pH or injected volume and concentration. However, no accurate information about the pathophysiological pathways involved can be drawn from these studies. The global skeletal muscle lesion has been described as a degenerative inflammatory process followed by regeneration through the proliferation and differentiation of myoblasts into adult myocytes (9). Although histological studies are useful for documenting the muscle tolerance of the various formulations under development, they are descriptive only of the cellular events occurring in the muscle. The acute hemodynamic events occurring in the injected muscle have recently been evaluated in the rabbit (10), and different pathways leading to the acute muscle damage described. Further documentation of the development of drug-induced muscle lesions at the molecular level would improve the understanding of the muscle reactions, and could lead to the development of new well-tolerated formulations.

The aim of the present study was to assess the gene expression profiles in control skeletal muscle and during the

PJF and LL contributed equally to this work and both should be considered as first authors.

[1] UMR181 de Physiopathologie et Toxicologie Expérimentales, INRA, ENVT, National Veterinary School, 23 chemin des Capelles BP 87614, Toulouse cedex 03 31076, France.
[2] UR 444 Cellular Genetics. INRA, Castanet-Tolosan France
[3] U466 Cell Regulation: Lipidoses and Atherosclerosis, Department of Pathology, INSERM, CHU Rangueil, Toulouse, France
[4] To whom correspondence should be addressed. (e-mail: h.lefebvre@envt.fr)

post-injury process in muscle from a non-rodent animal model at different times after an IM injection, in order to describe the whole molecular pathways, and to identify some new target genes involved in this pathophysiological situation. Propylene Glycol, a carrier solvent, was administered IM in piglets to induce a local muscle injury. A transcriptome analysis using cDNA microarrays was set up to evaluate the process of tissue injury and repair from the variation in expression of hundreds of genes that were examined over 21 days, along with the histological process.

MATERIALS AND METHODS

Animals and Husbandry

Ten crossbred male piglets ranging from 23 to 32 kg body weight at the onset of the acclimatization period (Bernussou, Villefranche de Rouergue, France) were used after being acclimated to the experimental conditions for two weeks.

The animals were kept at the National Veterinary School of Toulouse. They were provided with conventional starch food for piglets (Bernussou, Villefranche de Rouergue, France) and tap water *ad libitum*. They were observed daily throughout the experimental phase. The housing facilities had been approved by the French Ministry of Agriculture. All the experimental procedures were performed according to guide for the care and use of laboratory animals from the US National Institutes of Health. The study protocol had been reviewed and approved by the local ethical committee.

IM Injections of Propylene Glycol

Propylene Glycol (PG) was purchased from Sigma-Aldrich Chimie (Lyon, France). PG is commonly used as an organic solvent for topical or injectable pharmaceuticals (11), and it has been previously described as a model to induce post-injection muscle injury (12). The lumbar area of the animals was thoroughly shaved. A volume of 4 ml of PG was injected aseptically in a standardized manner using a 25 mm-long and 23-Gauge needle inserted perpendicularly to the lumbar area into the middle of the left or right *Longissimus dorsi* (LD) muscle. Each animal received a series of 4 IM injections of PG at five random sites in the left and right LD muscles at different time-intervals in order to obtain muscle lesions at different stages: the IM administrations were performed in the same animal at 6 h, and 2, 7 and 21 days before euthanasia. The additional fifth site did not receive any IM administration and was used as control non-injected muscle.

Muscle Sampling and Microscopic Examination

The piglets were euthanized using an overdose of pentobarbital (Dolethal, Vétoquinol, Lure, France). Samples from the muscle lesions and from control non-injected muscle were quickly excised in a standardized way and roughly cut up. The muscle samples for RNA isolation were immediately frozen in liquid nitrogen and stored at −80°C until analysis. The samples for the microscopic pathological examination, containing both normal and injured tissue, were immersed in standard buffered 4% formaldehyde solution. After fixation, they were dehydrated and embedded in paraffin. Slices of 3 μm thickness were obtained from each lesion and stained with hemalun-eosin and observed by a trained pathologist.

Total RNA Isolation

Total RNA was isolated from each of the 50 muscle samples (four injection sites per animal + one control non-injected site). Briefly, the muscle samples were disrupted, homogenized and ground to a fine powder by rapid agitation for 1 min in a liquid-nitrogen cooled grinder with stainless steel beads. An aliquot of 250–300 mg of the fine powder was then processed for total RNA isolation and purification using RNeasy® Fibrous Tissue Midi kit according to the manufacturers' instructions (Qiagen SA France, Courtaboeuf, France). The method included a proteinase K digestion step to remove proteins and a DNase digestion step to remove contaminating DNA. The extracted total RNA was eluted in 300 μl of RNase-free water and stored at −80°C. RNA quality and concentration were controlled using an AGILENT 2100 bioanalyzer (RNA solutions and RNA 6000 Nano LabChip Kit, Agilent Technologies France, Massy, France).

cDNA Arrays Design

Gene expression was analyzed by hybridization of nylon cDNA arrays (18×72 mm, Immobilon-NY+, Millipore, Bedford, MA) with radioactive probes. The arrays contained PCR products from 3,456 pig cDNA clones, spotted in duplicate on two separate fields of the same membrane with a Microgrid II fitted with a 32 pins microarray tool (BioRobotics MicroGrid, Genomic Solutions Ltd., Huntingdon, United Kingdom). The cDNA clones came mainly from a pig normalized multi-tissue cDNA library ("scag", Tosser-Klopp G, unpublished; 1,056 clones) and from a muscle library (Bendixen C, Department for Livestock Breeding and Genetics, Danish Institute of Agricultural Sciences, Tjele, Denmark; 2,208 clones). Other clones came from USDA MARC 1PIG and 2PIG libraries (13) and from the SENAH INRA laboratory (INRA-UMR SENAH, Domaine de la Prise, F 35590 Saint Gilles, France). Among these 3,456 clones, 1,651 corresponded to genes with an accession number and were only considered in the following analyses (MIAME standards, (14)). Sequences were annotated by BLAST analysis against SIGENAE contigs (Système d'information du projet d'analyse des génomes des animaux d'élevage, http://www.sigenae.org) and search for SWISSPROT features.

Hybridization of cDNA Arrays

The cDNA arrays were first hybridized with a vector oligonucleotide labeled with γ^{33}P-ATP at 42°C for 12 h to determine the quality of the spotting process. After washing, the arrays were exposed for 6 or 24 h to radioisotopic-sensitive imaging plates (BAS-2025, Fujifilm, Raytest France S.A.R.L., Courbevoie, France). The imaging plates were scanned thereafter with a phosphor imaging system at 25 μm resolution (BAS-5000, Fujifilm, Raytest France S.A.R.L.,

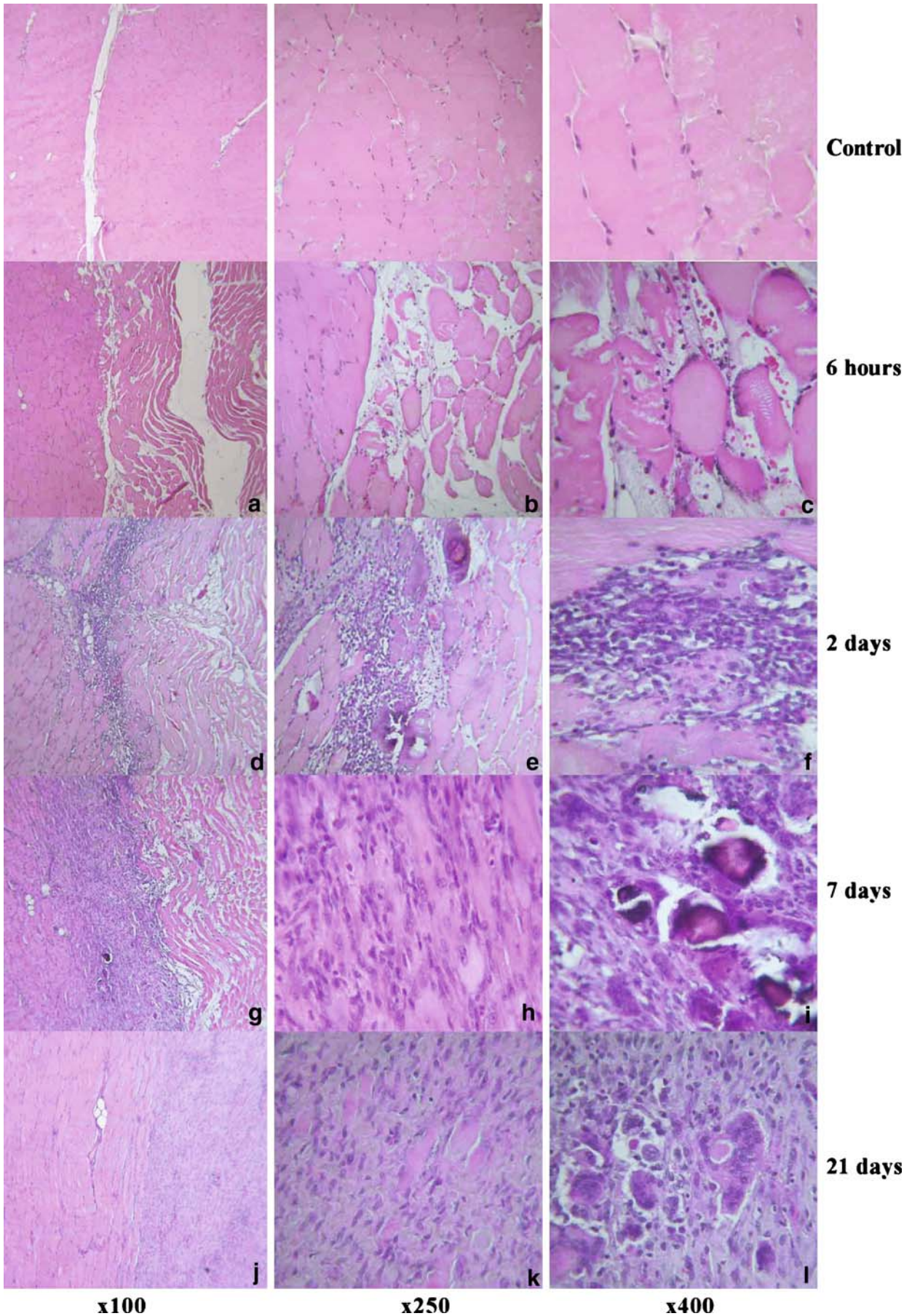
Control
6 hours
2 days
7 days
21 days
a
b
c
d
e
f
g
h
i
j
k
l
x100
x250
x400

Courbevoie, France). The arrays were then stripped and hybridized with a complex target. Briefly, cDNA was synthesized and labeled from 5 μg total RNA by simultaneous reverse transcription of mRNA using SuperScript™ II RNase H-Reverse Transcriptase (Invitrogen SARL, Life Technologies, Cergy Pontoise) and α–^{33}P-deoxy-CTP. The mRNA of each muscle sample was hybridized at 68°C for 24 h to a single array containing two duplicated separate fields. The hybridization images from vector and complex targets were quantified using the semi-automated software, BZScan (15). Fixed circle segmentation, i.e. a grid process with a fixed spot diameter was applied. The grid obtained with vector hybridization images was used to assess the reproducibility of the quantification signals between array replicates and also to analyze the complex target hybridization images. The complex hybridization images were quantified by extracting the intensity of each spot.

Data Analysis

Step 1. Data from the BZScan output were logarithmically transformed and the mean of the two duplicates calculated. Experimental variations in signal intensity between the 50 hybridizations were taken into account by normalizing, within each hybridization, the signal intensity for each spot by the average intensity of all the spots of the corresponding hybridization. The time-profile evolution of the expression of each mRNA was analyzed by calculating the differences in the quantified hybridization signals for each spot and for each animal between control non-injected muscle and the four consecutive time-conditions. Hence, four time-intervals were investigated, i.e.: 0–6 h, 6–48 h, 48 h–7 days, and 7–21 days.

Step 2. Two consecutive time conditions were compared for each spot by a paired-data Student's *t* test with the significance level set at 0.0125. In a second time, a ratio of at least 1.5 between two consecutive time-conditions was arbitrarily considered to demonstrate a significant increase or decrease in mRNA abundance. For each gene, at each time interval, the mRNA level could be stable, increased or decreased. Thus, taking together the variation of the mRNA level during the four successive defined time intervals, a global pattern of expression was then obtained over 21 days for each gene.

Step 3. A random Forest (RF) data analysis (16) was applied using R statistical software (R Development core team (2005), R: a language and environment for statistical computing, R Foundation for statistical computing, Vienna, Austria, http://www.cran.r-project.org). This approach has been used to identify predictors for prostate cancer tissue microarray data (17) and the methodology has been recently described for use in gene selection (18). Briefly, RF is a classification algorithm that performs a series of classification trees: For each classification tree, the overall data is cleaved in two groups, 2/3 sub-group is the learning data and the 1/3 sub-group is the testing data according to a random process for each sub-group and each tree. The genes are at the split decision and the samples are at the final allocation to a class. The learning data is used to build the classification tree and the testing data is used to verify if the expression of the genes gives a correct classification of the samples. During the testing process, the genes are permutated to test their importance or discriminant power for the classification. If a gene is important for a classification tree when it is permutated, the classification tree of the samples is lost. At the end, an aggregation process of the trees by majority vote gives a rank of importance for the genes. A total of 15,000 trees were performed, and 42 random inputs were attempted at each split. In the end, the first eight genes with the most discrimant power were selected.

Data Management

The experimental design, its implementation and the data handling complied with MIAME standards (14) and all the experimental data were managed using the free BASE software (19). A list of all the genes included in these microarrays and the normalized data have been deposited in the Gene Expression Omnibus database (http://www.ncbi.nlm.nih.gov/geo/) under GEO accession number GSE3217.

RESULTS

Pathological Findings

During muscle sampling, the muscle lesions, with a dark focal area in the case of acute lesions, and a white, dense and clearly identified scar in the late stages, could be easily distinguished from normal tissue. Both control non-injected muscle and muscle lesions are shown in Fig. 1.

Six hours after injection, the microscopical examination revealed prominent mechanical disruption of the myofibers along the junction between normal muscle and the injected area. Endomysial neutrophils and oedema were observed around the injured cells. At 2 days post-injection, the myocytes

◀ **Fig. 1.** Pathological examination of injured muscle. **a**, **d**, **g**, and **j** were taken at the same magnification ×100, with the injection area on the right side and normal muscle on the left. **b**, **e**, **h**, and **k** were taken at the same magnification ×250. **c**, **f**, **i**, and **l** were taken at the same magnification ×400. Control (non-injected) muscle images are shown at ×100, ×250 and ×400 magnifications. **abc**: 6 h after the IM injection. **a**: The area on the right side corresponds to myocytes that have been dissociated by the injected substance. **b**: Almost all the altered cells are located at the junction between the healthy and injured muscle tissue. **c**: Oedema and polynucleate (Check) cells surrounding the injured muscular cells are clearly observed. DEF: 2 days after the IM injection. **d**: Infiltrated lymphocytes are observed at the junction between the healthy and injured muscle tissue. **e**: Densification and hyalinisation of the injured cells is apparent. **f**: The cellular infiltrate is mainly composed of lymphocytes. **ghi**: 7 days after the IM injection. **g**: A thick fibro-inflammatory tissue layer has developed at the junction between the healthy and injured muscle tissue. **h**: This area contains fibroblast cells and regenerating but immature myocytes. **i**: Coagulated myocytes are being phagocytosed (Check)by giant cells. **jkl**: 21 days after the IM injection. **j**: Dense fibrous tissue is observed throughout the injected area. **k**: Some regenerating myocytes are observed. **l**: Giant cells containing some myocyte debris from the injected area remain in the centre of the injected area.

Table I. Gene Expression Patterns

Gene Expression Pattern				Gene Function	Gene Description (Gene name)
6h	2d	7d	21d		
↘	→	→	→	Metabolism	Fructose-bisphosphate aldolase A (ALDOA)
					Creatine kinase M (CKM)
					Glyceraldehyde-3-phosphate dehydrogenase (GAPD)
					Glycerol-3-phosphate dehydrogenase (GPD1)
					Pyruvate kinase, isozymes M1/M2 (PKM2)
					Phosphoglycerate mutase 2 (PGAM2)
					Glycogen phosphorylase, muscle (PYGM)
					Muscle type phosphofructokinase (M-PFK)
					Triosephosphate isomerase (TPI1)
				Mitochondrial metabolism	Cytochrome c oxidase subunit VIIa polypeptide 2 (COX7A2)
					Cytochrome c oxidase polypeptide VIII-heart (COX8H)
					NADH-ubiquinone oxidoreductase 19 kDa subunit (NDUFA8)
				Structure / Contraction	Actinin alpha 3 (ACTN3)
					Alpha-actin 1 (ACTA1)
					ATPase Ca++ transporting (ATP2A1, Skeletal muscle, fast twitch muscle (type II) fibers)
					Band 4.1-like protein 2 (EPB41L2)
					Myosin regulatory light chain 2 (Mylpf)
					Myosin binding protein C (MYBPC2)
					Myosin Heavy Chain (MYH1), MYH2, MYH4, MYH7
					Troponin C (TNNC2)
					Myozenin 1 (MYOZ1), Myozenin 3 (MYOZ3)
					Nebulin (NEB)
					Tropomyosin 1 (alpha) (TPM1)
					Tropomyosin 2 (beta) (TPM2)
				Nuclear activity	Carboxy-terminal domain RNA polymerase II polypeptide
					A small phosphatase 2 (CTDSP2 or OS4)
→	↘	→	→	Metabolism	ALDOA, CKM, PGAM2
					Enolase 3 (ENO3)
				Structure / Contraction	ACTA1, TNNC2, Mylpf, ATP2A1
→	→	↘	→	Metabolism	ALDOA, ENO3, CKM
↘	→	↘	→	Metabolism	ENO3
				Structure / Contraction	MYH4
				Unknown	FKSG26
↘	↘	→	→	Structure / Contraction	ACTN3
↘	→	→	→	Inflammation, immune reaction	Inhibitor of carbonic anhydrase precursor (ICA)
					Major seminal plasma glycoprotein (PSP1)
					NF-kappaB inhibitor-like protein 1 (NFKBIL1)
				Synaptic vesicle	Pantophysin (SYPL)
				Signal transduction	Annexin A5 (ANXA5)
					Glia maturation factor gamma (GMFG)
					Nucleoprotein (TPR)
					Tensin (TNS, signalling route JNK and p38 MAPK)
				Transcription/Translation	Trifunctional purine biosynthetic protein adenosine-3 (GART)
					tRNA synthase cofactor p38 (JTV1)
				Protein chaperone	Peptidyl-prolyl cis-trans isomerase like 2 (PPIL2),
					Heat shock 70 kDa protein 1 (HSPA1B)
				Protein interaction	Ankyrin repeat domain 6 (ANKRD6)
				Proteolysis	Carboxypeptidase D (CPD)
				Proliferation	BCL2-associated athanogene (BAG3, antiapoptotic)
				Unknown	C6orf134, C20orf160, KIAA0644
→	↗	→	→	Inflammation, immune reaction	Beta-2 microglobulin (B2M)
					Thymosin beta-4 (TMSB4)
					HLA-B associated transcript 1 (BAT1)
					Ferritin heavy polypeptide (FTH)
					Ferritin light polypeptide (FLH)
				Mitochondrial metabolism	Cytochrome c oxidase III (MTCO3)

					ATP synthase alpha chain, mitochondrial (ATP5A1)
				Structure	Tubulin alpha 1 (TUBA1), Cofilin 1 (CFL1)
				Protein synthesis	Translation elongation factor alpha (EEF1A1)
					Ribosomal proteins L8, L11, L18, L19, L23a, S3, S5, S11, S15, S19, S26
				Protein chaperone	Cyclophilin A (PPIA)
					Heat shock protein HSP 90-alpha (HSPCA)
				Proteolysis	Calpain small subunit 1 (CAPNS1)
					Legumain, protease cystein (LGMN)
				Unknown	C20orf178
→	→	↗	→	Inflammation, immune reaction	Complement cytolysis inhibitor or Clusterin (CLU)
				Proliferation	Osteonectin (SPARC)
				Extracellular matrix	Annexin A2 (ANXA2)
→	→	→	↗	Metabolism	Pyruvate kinase (PKM2)
				Proteolysis	Matrix metalloproteinase 2 (MMP2)
→	↗	↗	→	Structure	Collagen type 1 alpha 1(COL1A1)
					Fibronectin (FN1)
→	→	↗	↗	Extracellular matrix	Collagen type 1 alpha 2 (COL1A2)
↗	↘	→	→	Protein interaction	Ankyrin repeat domain 2 (ANKRD2)
				Signal transduction	Ras-related associated with diabetes (RRAD)
→	↗	↘	→	Structure	Desmin (DES)
↘	→	↗	→	Unknown	H19, imprinted maternally expressed untranslated mRNA

Gene expression patterns and detailed list of genes that were significantly differentially expressed during at least one of the time-intervals after IM injection of propylene glycol in porcine skeletal muscle: 0 h (control) to 6 h, from 6 h to 2 days, from 2 to 7 days, and then from 7 to 21 days. → = stable gene expression, ↗ = increased gene expression, ↘ = decreased gene expression

exhibited coagulation necrosis and the lymphocytes were clustered along the junction between the healthy and injured areas. At 7 days post-injection, the junction between these two areas consisted of a broad band of collagen containing regenerating myocytes. The final phase was observed at 21 days as a homogeneous fibrous and collagenous tissue invading the entire injected area, and maturing myocytes spreading from the periphery to the center of this area.

Validation of the Expression Data

The coefficient of variation calculated between all duplicate signals from vector and complex hybridization respectively were 19.5 and 18.9%. These results demonstrated the reliability of the whole process used in this study to generate expression data.

Identification of the Gene Expression Patterns

Out of the 1,651 genes, 324 were found to have a variable expression at the 0.0125 significance level. Among them, a total of 153 genes showed differential expression, i.e. under-or overexpression, with a ratio higher than 1.5, during at least one time interval. The expression was modified between control non-injected and 6 h after the IM injection for 54 genes, between 6 and 48 h for 41 genes, between 48 h and 7 days for 15 genes, and between 7 and 21 days for three genes.

The different gene expression patterns over time are presented in Table I. For each pattern, the genes are grouped in the table according to their main functions.

Most Discriminant Genes

The RF was used to classify genes according to their discriminant power, and the top eight genes were selected. Indeed, two selected genes had an increased level at 6 h: RRAD (GTP-binding protein RAD) and ANKRD2 (Ankyrin repeat domain protein 2), and six genes had an increased level between 2 and 21 days: SPARC (Secreted protein acidic and rich in cystein or Osteonectin), FN1 (Fibronectin), MMP2 (Matrix metalloproteinase-2), COL1A1 (Collagen alpha 1(I) chain), COL1A2 (Collagen alpha 2(I) chain) and TMSB4 (Thymosin beta-4). The individual expression data for these eight genes are presented in Fig. 2.

DISCUSSION

The strength of this study lies in the assessment of both histopathology and global gene expression profiles in a group of homogeneous animals in which the response of the same muscle to post-injection skeletal muscle injury could be studied within each animal at multiple time points. The major findings are that (1) Post-injection muscle injury is a complex pathophysiological situation involving several reaction pathways (2) the main changes in muscle gene expression occurred within the first 2 days, with a decrease of genes involved in muscle metabolism and contraction, and an increase of genes involved in inflammation, (3) the repairing process is concomitant with expression of genes involved in proteolysis, extracellular matrix development and myoblast activation, (4) such gene expression profiles are supported by pathological changes, and (5) these expression patterns were reproducible.

DNA microarray experiments have previously been used to address differences in gene expression profiles between various skeletal muscles, in studies of muscular metabolism in mice (20) and pig (21), ontogenesis in cattle (22), acute muscle reaction to freezing injury in mice (23), and several other muscular diseases. The pig was chosen here

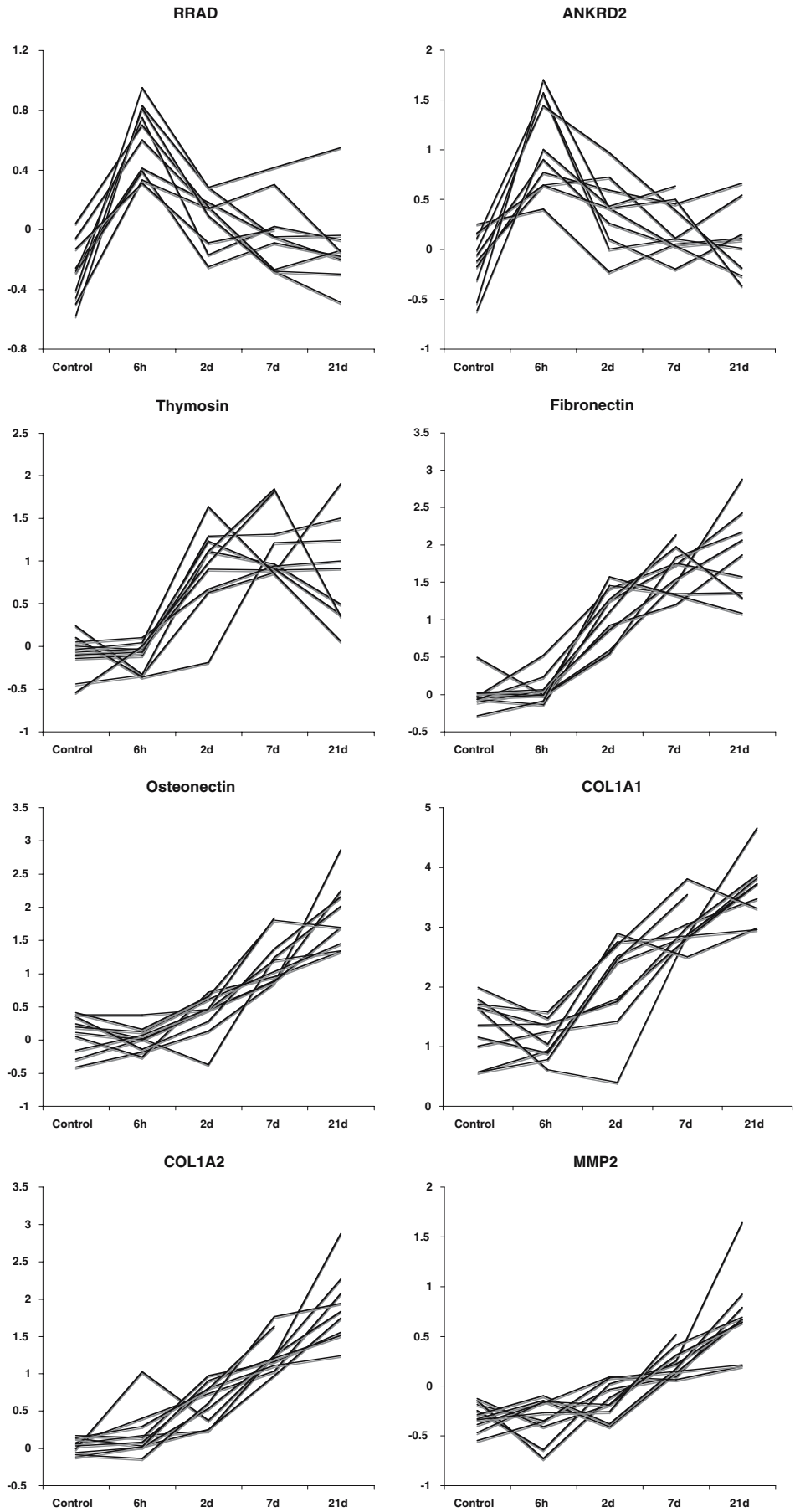
RRAD
1.2
0.8
0.4
0
-0.4
-0.8
Control
6h
2d
7d
21d
ANKRD2
2
1.5
1
0.5
0
-0.5
-1
Control
6h
2d
7d
21d
Thymosin
2.5
2
1.5
1
0.5
0
-0.5
-1
Control
6h
2d
7d
21d
Fibronectin
3.5
3
2.5
2
1.5
1
0.5
0
-0.5
Control
6h
2d
7d
21d
Osteonectin
3.5
3
2.5
2
1.5
1
0.5
0
-0.5
-1
Control
6h
2d
7d
21d
COL1A1
5
4
3
2
1
0
Control
6h
2d
7d
21d
COL1A2
3.5
3
2.5
2
1.5
1
0.5
0
-0.5
Control
6h
2d
7d
21d
MMP2
2
1.5
1
0.5
0
-0.5
-1
Control
6h
2d
7d
21d

as a non-rodent model for the histopathology and transcriptome analysis because of its homogeneous *Longissimus dorsi* muscle allowing several independent IM injections to be performed at different stages within the same individuals, hence reducing the response variability. The pig is also known for its particular sensitivity to post-injection muscle injury, and propylene glycol was selected as the irritant test article because previous studies had shown this organic co-solvent to be poorly tolerated by the skeletal muscle (12,24). By solely using a vehicle, instead of a drug formulation to induce the injury, any pharmacological effects that could have been related to an active substance was avoided.

The paired comparisons of gene expression between the consecutive stages of muscle injury were made longitudinally, which is rarely performed but improves the reliability of the analysis. This process highlighted the variation of expression in spite of differences in the individual basal expression levels. We focused here on the genes that were differentially expressed between consecutive time-intervals at both the selected significance level of 0.0125 and the differential expression ratio of at least 1.5. This approach reduced the risk of false discovery but probably also reduced the possibility of identifying the less variable genes. As new possible target genes were to be found, it was necessary to obtain the highest confidence in the identification of truly differentially expressed genes, rather than organizing all the investigated genes using traditional clustering approaches.

The gene expression data obtained here could be qualitatively analyzed with regard to results obtained for muscle degeneration and regeneration in other pathophysiological settings (9). The skeletal muscle is able to regenerate after injury due to a regulated balance of growth, fusion, and differentiation of the muscle precursor cells. Schematically, in a mechanically-induced muscle lesion, activated polymorphonuclear cells invade the injured area during the first 12 h and are followed by macrophages that remove the necrotic tissues within 2 days. Fibroblasts synthesize connective tissue while satellite cells become activated into myoblasts within the basal lamina. By day 7, the regenerating myoblasts have fused into myotubes, and by day 21, a scar with new myofibers and connective tissue has been formed (25). The histopathological findings in our study indicate that similar sequential events occur in porcine skeletal muscle after the induction by PG of local injury. It is also apparent from our study that muscle degeneration involved intracellular proteolysis, and started early with an increased expression of carboxypeptidase D followed at 48 h by the increased expression of calpain and legumain (cystein protease) transcripts. Concomitantly, the expression of genes encoding for the main structural and contractile muscle proteins as well as for the cellular and mitochondrial metabolism proteins, was decreased. This could be interpreted as a reduction of the muscle energy needs for contractile activities, since a degeneration period occurred immediately after the onset of injury. The gene for creatine kinase M, a specific muscular enzyme which is released into the plasma when muscle cells suffer, and is used as an index of muscle injury (26,27), was downregulated between control non-injected muscle and 6h muscle lesion. The genes encoding for the different ribosomal subunits were upregulated as early as 48 h after the IM injection. It probably resulted from activation of the quiescent satellite cells, and preceded the onset of protein synthesis that would later occur during the regeneration process. Indeed, muscle regeneration after an injury starts relatively rapidly, once the macrophages have phagocytosed the necrotic muscle fibers, and usually within 2 days (25). The fibroblasts seemed also to be involved in the formation of a scar at the injection site, since an increased transcription of different collagen subunits was observed from 48 h onwards. The tensin protein gene was activated from 6 h after injury. This gene is involved in muscle regeneration, as this process exhibits a 2-fold delay in KO mice (28). Desmin is an intermediate muscle-specific filament protein which is expressed in proliferating myoblasts as early as 12 h after muscle injury. It is increased later and is used as an index of skeletal muscle regeneration. The expression of desmin genes was increased during the time interval from 48 h to 7 days after injection, which is consistent with early muscular regeneration. In contradiction to the classical models which describes successive steps of necrosis, inflammation and regeneration, our expression data also clearly suggest that these processes occur simultaneously. This is in accordance with the pathological examination which revealed the development of a thick layer of fibro-inflammatory tissue next to the necrotic area, leading to muscle regeneration.

Using the Random Forest method, the genes were sorted according to their discriminant power without the need to refer to arbitrary thresholds to rank the genes, and the top eight genes were selected (18). This non parametric method is particularly adapted to data with many more genes (variables) than samples, and even to correlated variables. The two genes up-regulated at 6 h were RRAD and ANKRD2. RRAD codes for a cytoplasmic protein involved in signal transduction and ANKRD2, a putative muscle-specific myogenic regulator (29), codes for a cytoplasmic protein interacting with p53 transcriptional factor (30,31). The six genes up-regulated from 2 days or later after IM code for proteins involved in myogenic cell migration and in the extracellular matrix remodeling during muscle tissue repair. The gene expression of two collagens (COL1A1 and COL1A2), fibronectin (FN1) and matrix metalloproteinase (MMP2) was closely related to the fibrogenic tissue development clearly visible in the pathological examination. Expression of the matricellular SPARC protein is restricted to tissues that undergo consistent turnover or to sites of injury and disease (32,33). Another microarray analysis also identified MMP2, SPARC and COL1A2 as being over-expressed during development of fibrosis in radiation-induced enteritis (34). Thymosin β4 acts as an anti-inflammatory agent (35) and its expression was abruptly up-regulated between 6 and 48 h. Thymosin β4 also accelerates wound healing (36). Further experiments should explore the possibility of using these discriminant genes as markers of the repair process and of evaluating any complications of the muscle lesions due to fibrosis.

Muscle reaction to IM administration has been shown in the present study to be complex, involving multiple reaction

◀ **Fig. 2.** Expression data for each animals for the eight most discriminant genes. Each gene is represented in one individual sub-figure, and each animal is represented by one single plot. Normalized values of gene expression levels (*y*-axis) are expressed for each time-condition (*x*-axis: control muscle, 6 h, 2 days, 7 days and 21 days lesions).

pathways, with a large number of genes significantly down or upregulated over 21 days. However, on the whole and as summarized in Table I only 14 different patterns of gene expression profile were encountered. This is far from the total number of all the possible patterns, *ie* 81, or 3^4 (the expression level of each gene may indeed increase, decrease or may be at a constant level at each of the four time intervals). This total number of patterns was theoretically possible but not biologically relevant, since our data showed that only 17% (14/81) of the theoretical patterns were found. This suggest that the pathophysiological reaction observed in this study at the molecular level is not anarchic but rather well organized. Several concomitant pathways had been already observed in a short term evaluation of the muscle blood flow response during the first 6 h following the IM administration, and the inhibition of each pathway induced a decrease in the observed blood flow, with or without reduction of the actual muscle injury (10). Similarly, in the current study about long-term muscle reaction, it is unclear which of the reaction pathways would be to inhibit or to enhance in order to ameliorate muscle healing. Indeed, proteolysis might be detrimental to the muscle for a transient period, but in many pathophysiological settings, it might be a favourable cleaning process that is a pre-requisite for muscle healing.

In conclusion, this study illustrated the relevance of longitudinal microarray data analysis within the same subjects. This porcine model of post-injection muscle injury offers a good model for assessing gene expression of different types of muscle lesions (especially acute vs. chronic) within the same subjects, and might be used to investigate other pathophysiological settings in muscle.

Several variable genes involved mainly in inflammation, energy metabolism and cytoskeleton organization were identified. Thus post-injection muscle injury must be considered as multifactorial. However, the muscle reaction is not anarchic but a rather organized phenomenon since only a limited number of gene expression profile patterns was observed. This organization of molecular events associated with the development of muscle damage implies that it might be possible to control this development pharmacologically. To date, no straightforward and univocal solution can be proposed to improve or predict the tolerance of drug formulations, but understanding the underlying signaling pathways at the molecular level could provide new knowledge for potential modulation of the resulting muscle damage. Another relevant investigation would be to compare several different vehicles using the same model, in an attempt to identify the prevailing patterns of gene expression profiling.

Eight genes were shown to be the most discriminant in muscle damage development. Further investigations are needed to assess the relationship between the expressions of these genes and lesion severity, but they might serve as useful biomarkers to assess muscle tolerance of a drug vehicle or formulation in the future.

ACKNOWLEDGEMENTS

The muscle specific cDNA library used in this work was kindly provided by Christian Bendixen. The authors thank Rémi Houlgatte (TAGC, Marseille, France) for critical discussions about/on Nylon microarray methodology and data analysis. We thank Jean-Pierre Gau, Nadine Gautier, Francis Benne, and Janine Rallières for their technical assistance. We wish to acknowledge support from the CRGS platform of the Toulouse Midi-Pyrenees Genopole (Cécile Donnadieu-Tonon) (http://genopole-toulouse.prd.fr/), where the nylon membranes were produced. The database with BASE software for MIAME submission was developed by Christelle Dantec and managed by a computer group (SIGENAE, Système d'information du projet d'analyse des génomes des animaux d'élevage, http://www.sigenae.org). We thank the work group for statistical analysis of microarray data (Philippe Besse, Alain Baccini, Sébastien Déjean, http://www.lsp.ups-tlse.fr/Programmes/Biopuces/) for their advice in the RF analysis and to Christèle Robert-Granié for helpful discussions on the statistical methods.

REFERENCES

1. L. F. Hill. Sites for intramuscular injections. *J. Pediatr.* **70**:158–159 (1967).
2. D. J. Greenblatt and M. D. Allen. Intramuscular injection-site complications. *Jama* **240**:542–544 (1978).
3. P. C. Beecroft and S. Redick. Possible complications of intramuscular injections on the pediatric unit. *Pediatr. Nurs.* **15**:333–336 (1989).
4. E. V. Alvarez, M. Munters, L. S. Lavine, H. Manes, and J. Waxman. Quadriceps myofibrosis. A complication of intramuscular injections. *J. Bone Joint Surg. Am.* **62**:58–60 (1980).
5. S. S. Babhulkar. Triceps contracture caused by injections. A report of 11 cases. *J. Bone Joint Surg. Br.* **67**:94–96 (1985).
6. P. S. Bergeson, S. A. Singer, and A. M. Kaplan. Intramuscular injections in children. *Pediatrics* **70**:944–948 (1982).
7. L. Rossi and D. Conen. Intramuscular injections—an outdated form of administration? 6 cases of Staphylococcus aureus sepsis following intramuscular injections. *Schweiz. Med. Wochenschr.* **125**:1477–1482 (1995).
8. R. K. Gherardi, M. Coquet, P. Cherin, L. Belec, P. Moretto, P. A. Dreyfus, J. F. Pellissier, P. Chariot, and F. J. Authier. Macrophagic myofasciitis lesions assess long-term persistence of vaccine-derived aluminium hydroxide in muscle. *Brain* **124**:1821–1831 (2001).
9. J. G. Tidball. Inflammatory processes in muscle injury and repair. *Am. J. Physiol. Regul. Integr. Comp. Physiol.* **288**:R345–R353 (2005).
10. P. J. Ferre, E. Thein, I. Raymond-Letron, P. L. Toutain, and H. P. Lefebvre. Acute changes in muscle blood flow and concomitant muscle damage after an intramuscular administration. *Pharm. Res.* **22**:405–412 (2005).
11. F. Mottu, A. Laurent, D. A. Rufenacht, and E. Doelker. Organic solvents for pharmaceutical parenterals and embolic liquids: a review of toxicity data. *PDA J. Pharm. Sci. Technol.* **54**:456–469 (2000).
12. G. A. Brazeau and H. L. Fung. Mechanisms of creatine kinase release from isolated rat skeletal muscles damaged by propylene glycol and ethanol. *J. Pharm. Sci.* **79**:393–397 (1990).
13. S. C. Fahrenkrug, T. P. Smith, B. A. Freking, J. Cho, J. White, J. Vallet, T. Wise, G. Rohrer, G. Pertea, R. Sultana, J. Quackenbush, and J. W. Keele. Porcine gene discovery by normalized cDNA-library sequencing and EST cluster assembly. *Mamm. Genome* **13**:475–478 (2002).
14. A. Brazma, P. Hingamp, J. Quackenbush, G. Sherlock, P. Spellman, C. Stoeckert, J. Aach, W. Ansorge, C. A. Ball, H. C. Causton, T. Gaasterland, P. Glenisson, F. C. Holstege, I. F. Kim, V. Markowitz, J. C. Matese, H. Parkinson, A. Robinson, U. Sarkans, S. Schulze-Kremer, J. Stewart, R. Taylor, J. Vilo, and M. Vingron. Minimum information about a microarray experiment (MIAME)-

toward standards for microarray data. *Nat. Genet.* **29**:365–371 (2001).
15. F. Lopez, J. Rougemont, B. Loriod, A. Bourgeois, L. Loi, F. Bertucci, P. Hingamp, R. Houlgatte, and S. Granjeaud. Feature extraction and signal processing for nylon DNA microarrays. *BMC Genomics* **5**:38 (2004).
16. L. Breiman. Random forests. *Mac. Learn.* **45**:5–32 (2001).
17. D. B. Seligson, S. Horvath, T. Shi, H. Yu, S. Tze, M. Grunstein, and S. K. Kurdistani. Global histone modification patterns predict risk of prostate cancer recurrence. *Nature* **435**:1262–1266 (2005).
18. R. Diaz-Uriarte, and S. Alvarez de Andres. Gene selection and classification of microarray data using random forest. *BMC Bioinformatics* **7**:3 (2006).
19. L. H. Saal, C. Troein, J. Vallon-Christersson, S. Gruvberger, A. Borg, and C. Peterson. BioArray Software Environment (BASE): a platform for comprehensive management and analysis of microarray data. *Genome. Biol.* **3**:SOFTWARE0003 (2002).
20. W. G. Campbell, S. E. Gordon, C. J. Carlson, J. S. Pattison, M. T. Hamilton, and F. W. Booth. Differential global gene expression in red and white skeletal muscle. *Am. J. Physiol. Cell Physiol.* **280**:C763–C768 (2001).
21. Q. Bai, C. McGillivray, N. da Costa, S. Dornan, G. Evans, M. J. Stear, and K. C. Chang. Development of a porcine skeletal muscle cDNA microarray: analysis of differential transcript expression in phenotypically distinct muscles. *BMC Genomics* **4**:8 (2003).
22. K. Sudre, C. Leroux, G. Pietu, I. Cassar-Malek, E. Petit, A. Listrat, C. Auffray, B. Picard, P. Martin, and J. F. Hocquette. Transcriptome analysis of two bovine muscles during ontogenesis. *J. Biochem. (Tokyo)* **133**:745–756 (2003).
23. M. Summan, M. McKinstry, G. L. Warren, T. Hulderman, D. Mishra, K. Brumbaugh, M. I. Luster, and P. P. Simeonova. Inflammatory mediators and skeletal muscle injury: a DNA microarray analysis. *J. Interferon. Cytokine Res.* **23**:237–245 (2003).
24. G. A. Brazeau and H. L. Fung. Use of an *in vitro* model for the assessment of muscle damage from intramuscular injections: *in vitro–in vivo* correlation and predictability with mixed solvent systems. *Pharm. Res.* **6**:766–771 (1989).
25. T. Hurme, H. Kalimo, M. Lehto, and M. Jarvinen. Healing of skeletal muscle injury: an ultrastructural and immunohistochemical study. *Med. Sci. Sports Exerc.* **23**:801–810 (1991).
26. H. P. Lefebvre, V. Laroute, J. P. Braun, V. Lassourd, and P. L. Toutain. Non-invasive and quantitative evaluation of post-injection muscle damage by pharmacokinetic analysis of creatine kinase release. *Vet. Res.* **27**:343–361 (1996).
27. P. J. Ferre, D. Concordet, V. Laroute, G. P. Chanoit, J. P. Ferre, M. Manesse, and H. P. Lefebvre. Comparison of ultrasonography and pharmacokinetic analysis of creatine kinase release for quantitative assessment of postinjection muscle damage in sheep. *Am. J. Vet. Res.* **62**:1698–1705 (2001).
28. A. Ishii and S. H. Lo. A role of tensin in skeletal-muscle regeneration. *Biochem. J.* **356**:737–745 (2001).
29. C. Bean, M. Salamon, A. Raffaello, S. Campanaro, A. Pallavicini, and G. Lanfranchi. The Ankrd2, Cdkn1c and calcyclin genes are under the control of MyoD during myogenic differentiation. *J. Mol. Biol.* **349**:349–366 (2005).
30. S. Kojic, E. Medeot, E. Guccione, H. Krmac, I. Zara, V. Martinelli, G. Valle, and G. Faulkner. The Ankrd2 protein, a link between the sarcomere and the nucleus in skeletal muscle. *J. Mol. Biol.* **339**:313–325 (2004).
31. A. Pallavicini, S. Kojic, C. Bean, M. Vainzof, M. Salamon, C. Ievolella, G. Bortoletto, B. Pacchioni, M. Zatz, G. Lanfranchi, G. Faulkner, and G. Valle. Characterization of human skeletal muscle Ankrd2. *Biochem. Biophys. Res. Commun.* **285**:378–386 (2001).
32. A. D. Bradshaw and E. H. Sage. SPARC, a matricellular protein that functions in cellular differentiation and tissue response to injury. *J. Clin. Invest.* **107**:1049–1054 (2001).
33. R. A. Brekken and E. H. Sage. SPARC, a matricellular protein: at the crossroads of cell-matrix. *Matrix Biol.* **19**:569–580 (2000).
34. C. Strup-Perrot, D. Mathe, C. Linard, D. Violot, F. Milliat, A. Francois, J. Bourhis, and M. C. Vozenin-Brotons. Global gene expression profiles reveal an increase in mRNA levels of collagens, MMPs, and TIMPs in late radiation enteritis. *Am. J. Physiol. Gastrointest. Liver Physiol.* **287**:G875–G885 (2004).
35. J. D. Young, A. J. Lawrence, A. G. MacLean, B. P. Leung, I. B. McInnes, B. Canas, D. J. Pappin, and R. D. Stevenson. Thymosin beta 4 sulfoxide is an anti-inflammatory agent generated by monocytes in the presence of glucocorticoids. *Nat. Med.* **5**:1424–1427 (1999).
36. K. M. Malinda, G. S. Sidhu, H. Mani, K. Banaudha, R. K. Maheshwari, A. L. Goldstein, and H. K. Kleinman. Thymosin beta4 accelerates wound healing. *J. Invest. Dermatol.* **113**:364–368 (1999).